*Macromolecules* **1998,** *31,* 4695−4702

# Acrylonitrile and Glycidyl Methacrylate Copolymers: Nuclear Magnetic Resonance Characterization

**A. S. Brar* and Kaushik Dutta**

*Department of Chemistry Indian Institute of Technology, Delhi Hauz Khas, New Delhi 110 016, India*

*Received February 6, 1998; Revised Manuscript Received May 8, 1998*

ABSTRACT: Copolymers containing acrylonitrile (A) and glycidyl methacrylate (G) units of different compositions were synthesized by free radical solution polymerization. The reactivity ratios were estimated by Kelen Tudos and nonlinear error in variable methods. The triad sequence distributions in terms of A- and G-centered triads have been obtained from $^{13}C\{^1H\}$ NMR spectroscopy. The complete spectral assignments in terms of compositional and configurational sequences of the overlapping carbon and proton spectra of these copolymers were done with the help of distortionless enhancement by polarization transfer (DEPT), two-dimensional proton-detected heteronuclear correlation (inverse-HETCOR), and total correlated spectroscopy (TOCSY) experiments. The Monte Carlo simulation was used to study the effect of the fractional conversion on the triad fractions.

## Introduction

Acrylonitrile-based copolymers have many commercial applications.[1] The need for functional polymers for several specialty applications demands the synthesis of these materials with well-controlled structures and topologies.[2,3] The copolymers based on the glycidyl methacrylate belong to the potential class of functional polymers. The interest in these copolymers is largely due to the ability of the pendent epoxy group to enter into a large number of chemical reactions,[4,5] thus offering the opportunity for chemical modification of the parent copolymer for various applications. The knowledge of microstructure is essential to understand the macroscopic characterization of the polymers. Two-dimensional NMR spectroscopy has been used for determining the compositional[6−8] and configurational[9−11] sequences of the polymers. The microstructure of poly(glycidyl methacrylate) and its copolymers with alkyl acrylates, *N*-vinylpyrrolidione, vinyl acetate, etc. have been investigated by many workers.[12−14] The microstructure of acrylonitrile copolymers with alkyl methacrylates has been reported earlier.[15a−e] To the best of our knowledge the microstructure of acrylonitrile/glycidyl methacrylate (A/G) copolymers has not been reported so far.

In this paper, we report the copolymerization mechanism of industrially important acrylonitrile/glycidyl methacrylate copolymers prepared by solution polymerization. The overlapping carbon-13 NMR spectra of the A/G copolymers were assigned without ambiguity, with the help of DEPT experiments. The methine, methylene, and α-methyl carbon signals of the A/G copolymers were sensitive to compositional and configurational sequences. The various compositional/configurational sequences were assigned to triad, tetrad, and pentad sequences with the help of the inverse-HETCOR (HSQC) and DEPT experiments. 2D inverse-HETCOR and TOCSY (low mixing time) experiments were used for complete assignments of the overlapping and broad proton spectra of the A/G copolymers. The reactivity ratios of the comonomers were estimated using the Kelen Tudos[16] (KT) and nonlinear error-in-variable[17] (EV) methods. The triad sequence distribution in terms of A and G units were obtained from the $^{13}C\{^1H\}$ NMR spectra of the copolymers. The Monte Carlo (MC) simulation method[18] was used to study the effect of the triad fraction as a function of fractional conversion.

## Experimental Section

Acrylonitrile (GSC) and glycidyl methacrylate (Merck) were distilled under reduced pressure and stored below 5 °C. A series of A/G copolymers containing different mole fractions of acrylonitrile in the feed were prepared by solution polymerization using benzoyl peroxide as initiator. The percent conversion was kept around 5−6% by precipitating the copolymers in methanol. The copolymers were further purified from the DMSO/methanol system. The copolymer composition was calculated from the percent nitrogen of the copolymers. The C, H, and N analyses were done on a Perkin-Elmer 240C elemental analyzer instrument.

NMR experiments were performed in DMSO-$d_6$ on a Bruker DPX-300 spectrometer at a frequency of 300.13 and 75.7 MHz for $^1H$ and $^{13}C\{^1H\}$ NMR spectra, respectively. DEPT measurements were carried out in DMSO-$d_6$ at 100 °C using the standard pulse sequence with a $J$ modulation time of 3.7 ms ($J_{CH} = 135$ Hz) with 2 s delay time. The two-dimensional proton-detected heteronuclear chemical shift correlation experiment (inverse-HETCOR) was recorded in DMSO-$d_6$ at 100 °C using the standard pulse sequence.[19] A total of 32 scans were accumulated with a relaxation delay of 2 s for each of the 512 $t_1$ experiments. The two-dimensional homonuclear total correlation spectroscopy (TOCSY) spectrum was recorded at 4 ms mixing time in DMSO-$d_6$ at 100 °C. A total of 32 scans were accumulated with a relaxation delay of 2 s for each of the 512 $t_1$ experiments. The details of the Lorentzian shape curve fitting have been described elsewhere.[7] All regression converged to $\chi^2 < 1$.

## Results and Discussion

**Monomer Reactivity Ratios.** The copolymer composition of acrylonitrile/glycidyl methacrylate (A/G) copolymers were determined from the percent nitrogen in the copolymers using the following equation:

$$F_A = \frac{M_G N}{M_G N + 1400 - M_A N}$$

---

* To whom all correspondence should be addressed.

S0024-9297(98)00184-3 CCC: $15.00

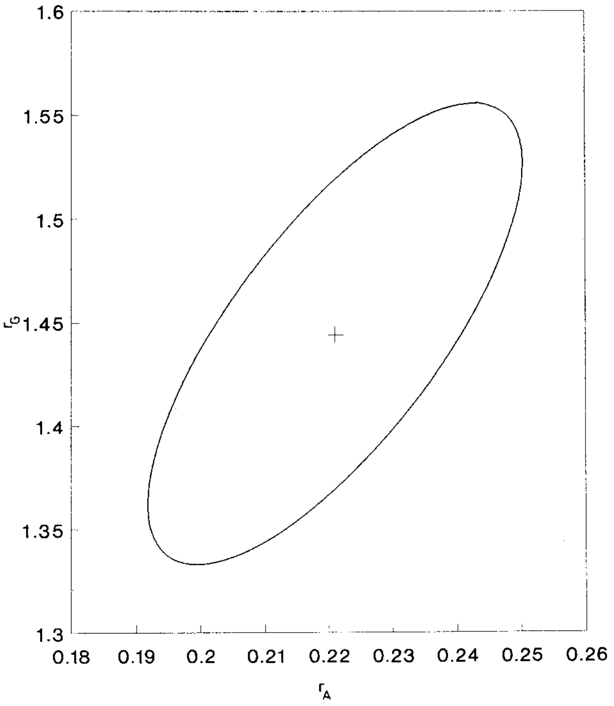

**Figure 1.** 95% joint confidence interval contour plot for the acrylonitrile/glycidyl methacrylate (A/G) comonomer pair.

where $M_A$ and $M_G$ are the molecular weight of acrylonitrile and glycidyl methacrylate and $N$ is the percent nitrogen in the copolymer.

The copolymer composition data, calculated from nitrogen analysis, were used to calculate the terminal model reactivity ratios using the nonlinear least-squares error-in-variable (EV) method. The terminal model reactivity ratios calculated from the KT method ($r_A$ = 0.21 and $r_G$ = 1.37) served as the initial estimate for the calculation of reactivity ratios by the EV method. The reactivity ratios obtained from the EV method are $r_A$ = 0.22 and $r_G$ = 1.44. A 95% joint confidence interval plot for the A/G comonomer pair is shown in Figure 1. Using the van Herk[20] method, the sum of squares of the residuals for different reactivity ratios was plotted. From the plot, the minimum was obtained for $r_A$ = 0.22 and $r_G$ = 1.47 with a relative sum of squares of 0.0018. The terminal model reactivity ratios obtained from the EV method ($r_A$ = 0.22 and $r_G$ = 1.44) are in excellent agreement with the values calculated by the van Herk method. Examination of the residuals showed that there is no systematic variation and that the actual deviation of the data with respect to the fitted ($F_A$) values are not bigger than the expected errors, thus indicating that the reactivity ratios obtained from the compositional data (nitrogen analysis) are reliable.

**$^{13}C\{^1H\}$ NMR and $^1H$ NMR Studies.** The $^{13}C\{^1H\}$ NMR spectrum of the A/G copolymer ($F_A$ = 0.48) in DMSO-$d_6$ is shown in Figure 2. The carbonyl and nitrile carbon resonances are around $\delta$ 173.2−177.0 and 119.0−124.0 ppm, respectively. Both of these carbon signals showed multiplets, indicating that they are sensitive to the compositional sequences and can be used for the assessment of the copolymerization mechanism. The spectral region $\delta$ 10.0−70.0 ppm is very complex and overlapping and can be assigned to aliphatic carbons in the main and side chains of the copolymers. The extent of overlap of the various carbon signals cannot be ascertained from the $^{13}C\{^1H\}$ NMR spectroscopy. The overlapping carbon regions can be resolved by employing the DEPT-135 NMR (Figure 3), where the methylene carbon signal is negative and the methine and methyl carbon signals are positive. The $-OCH_2$, epoxy methylene $(CH_2)_e$, and epoxy methine $(CH)_e$ carbon signals are assigned around $\delta$ 65.48, 44.09, and 48.61 ppm, respectively. The $\beta$-methylene carbon of both A and G units resonates around $\delta$ 30.0−55.0 ppm. The methine and methyl carbon signals are overlapping with

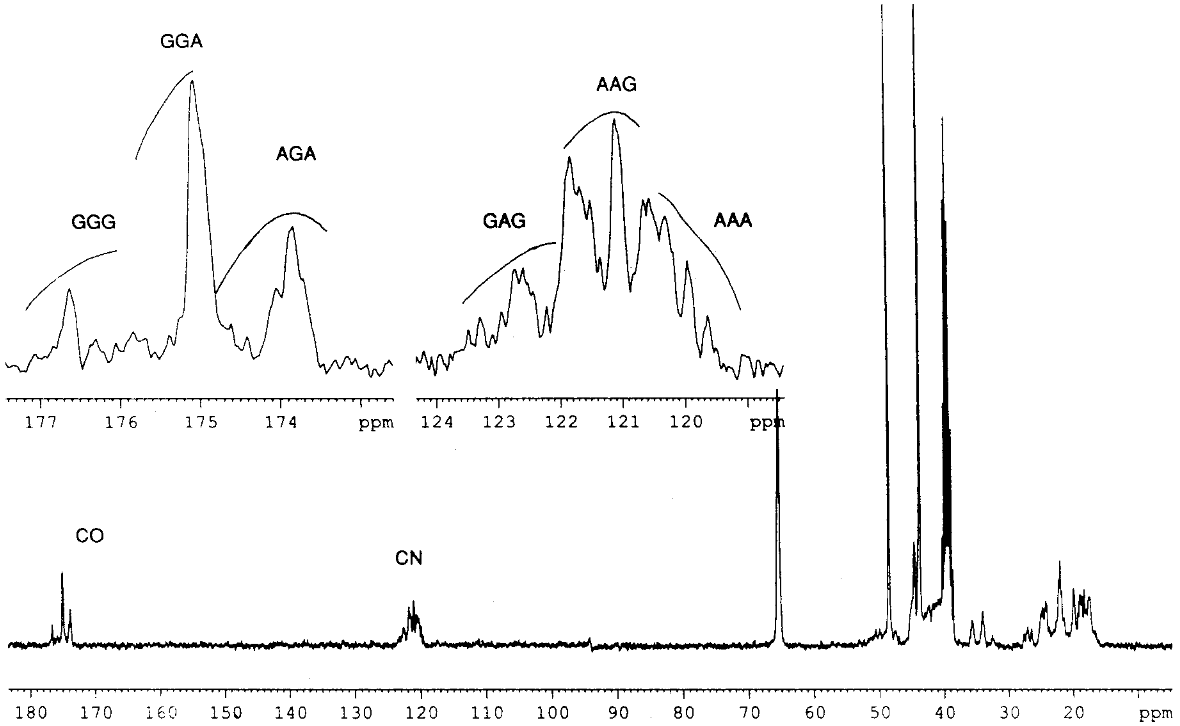

**Figure 2.** 75.5 MHz $^{13}C\{^1H\}$ NMR spectrum of the acrylonitrile/glycidyl methacrylate copolymer ($F_A$ = 0.48) along with expanded carbonyl and nitrile carbon resonances in DMSO-$d_6$.

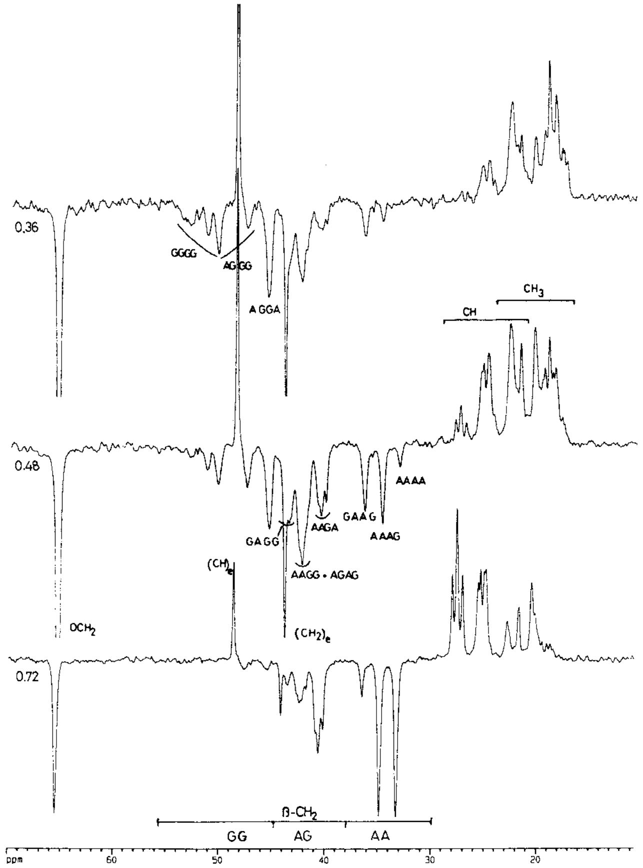

**Figure 3.** 135-DEPT spectrum of acrylonitrile/glycidyl methacrylate copolymer recorded in DMSO-$d_6$ at 100 °C.

each other and can be resolved by the DEPT-90 experiment, where only the methine signals are detected. The signals around $\delta$ 21.0−29.0 ppm are assigned to methine carbon resonances, whereas the methyl carbon resonances are assigned around $\delta$ 16.0−24.0 ppm (Figure 3).

The methine carbon resonances are sensitive to compositional and configurational sequences. DEPT-90 spectra of different copolymer compositions for A/G copolymers are shown in Figure 4. The methine carbon region is divided into three broad envelopes. In the homopolymer, poly(acrylonitrile) (PAN), the three signals in the methine carbon region ($\delta$ 26.5−28.5 ppm) are assigned to ArArA, AmArA/ArAmA, and AmAmA tacticity from low to high field.[21] On comparison with the homopolymer, PAN, the methine signals in the region $\delta$ 26.5−28.5 ppm, which decrease in intensity as the acrylonitrile content in the copolymer decreases, therefore are assigned to the AAA triad fraction. In the AAA region, the three signals at $\delta$ 27.96, 27.55, and 26.97 ppm are assigned to ArArA, AmArA (ArAmA), and AmAmA tacticity, respectively, as assigned for the homopolymer PAN. The methine carbon signals around $\delta$ 23.5−26.5 and 21.0−23.5 ppm, are assigned to AAG and GAG triad fractions, respectively, on the basis of the change in intensity of the signals with copolymer composition. Further splitting within these triad fractions can be assigned to compositional sequences.

In the AAG triad region the three multiplets are assigned to pentad compositional sequences on the basis of the change in intensity of the signals with composition. The three signals around $\delta$ 25.0−26.5, 24.4−25.0, and 24.24 ppm are assigned to AAAGA, AAAGG + GAAGA, and GAAGG pentads, respectively (Figure 4). Further splittings within the AAAGA pentad sequences, which do not change with the copolymer composition are due to configurational sensitivity. The signals at $\delta$ 25.45 and 25.24 ppm are assigned to AArAGA and AAmAGA, respectively, because of the different configurational arrangements of the A unit in the central AAG triad. The signals at $\delta$ 24.92 and 24.76 ppm are assigned to AAAGG and GAAGA pentads, respectively. In the GAG region, the three clear signals, which show variation with the copolymer composition, at $\delta$ 22.70, 22.49, and 22.1−21.0 ppm are assigned to AGAGA, AGAGG, and GGAGG pentad sequences, respectively (Figure 4).

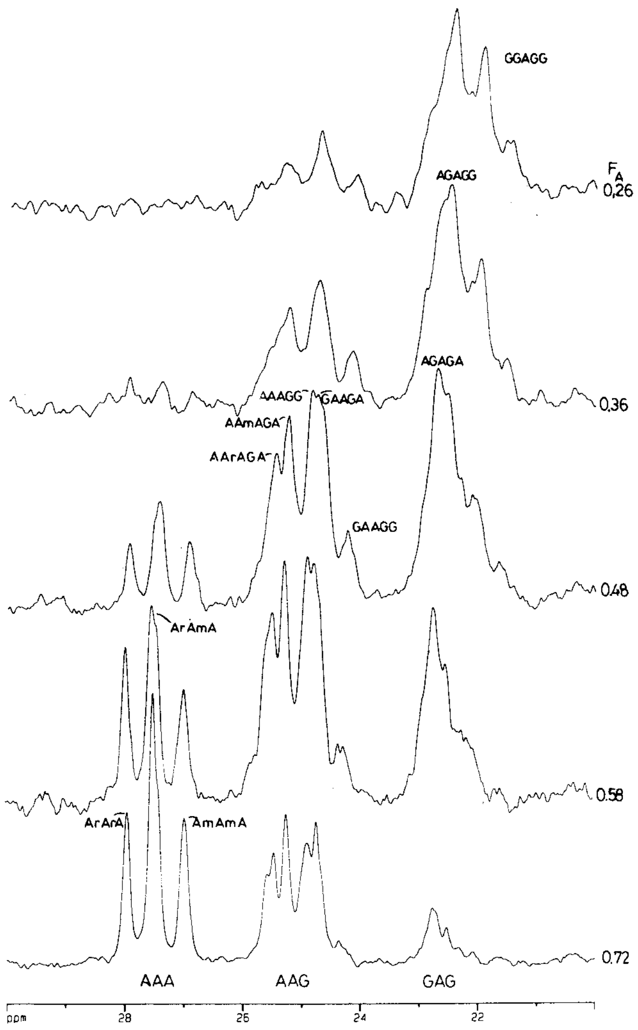

**Figure 4.** DEPT-90 spectra showing the methine carbon signals of A/G copolymers of different compositions in DMSO-$d_6$ at 100 °C.

The methylene carbon, due to its symmetry, is sensitive to diad, tetrad, hexad, etc. compositional sequences. The methylene carbon signals can be divided into three envelopes of multiplets, which change with the copolymer composition, and are assigned to diads AA ($\delta$ 32.0−38.0 ppm), AG (GA) ($\delta$ 38.5−44.6 ppm), and GG ($\delta$ 44.6−55.0 ppm), as shown in Figure 3. The additional signals within each diad, which change in intensity with copolymer composition, can be assigned to tetrad and hexad compositional sequences with the help of inverse-HETCOR spectra (Figure 5a,b). The three signals in the AA diad region, which vary with the copolymer composition, are assigned to AAAA ($\delta$ 33.27 ppm),

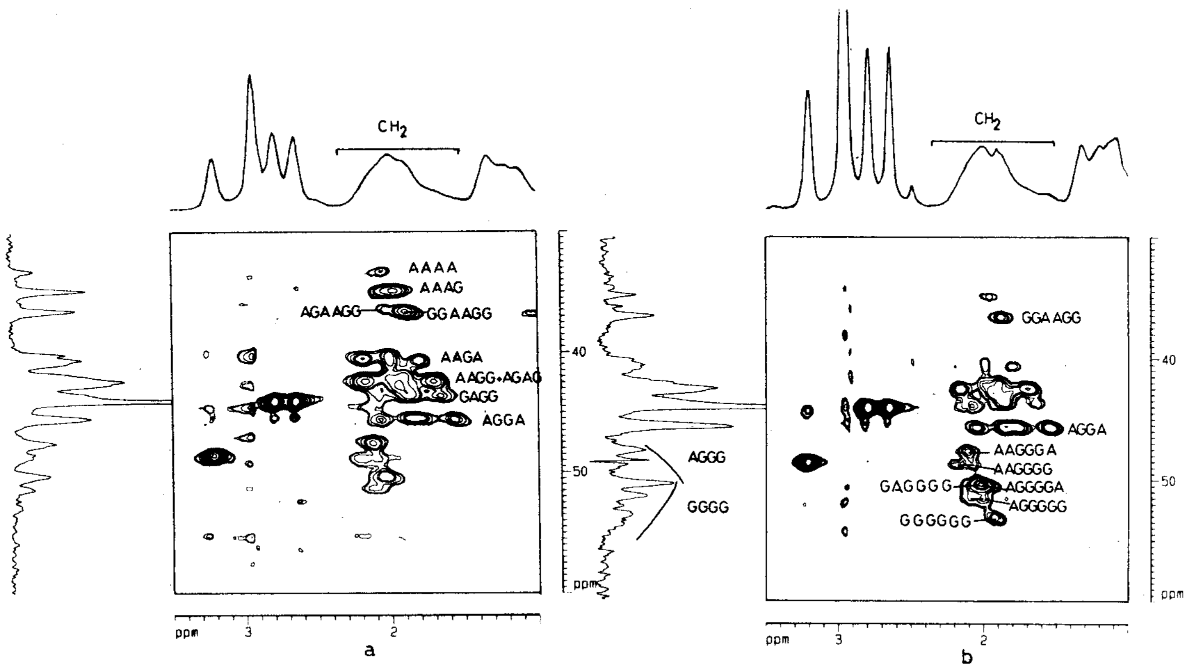

**Figure 5.** Methylene region of the inverse-HETCOR spectrum of A/G copolymers (a) $F_A = 0.48$ and (b) $F_A = 0.36$ in DMSO-$d_6$ at 100 °C.

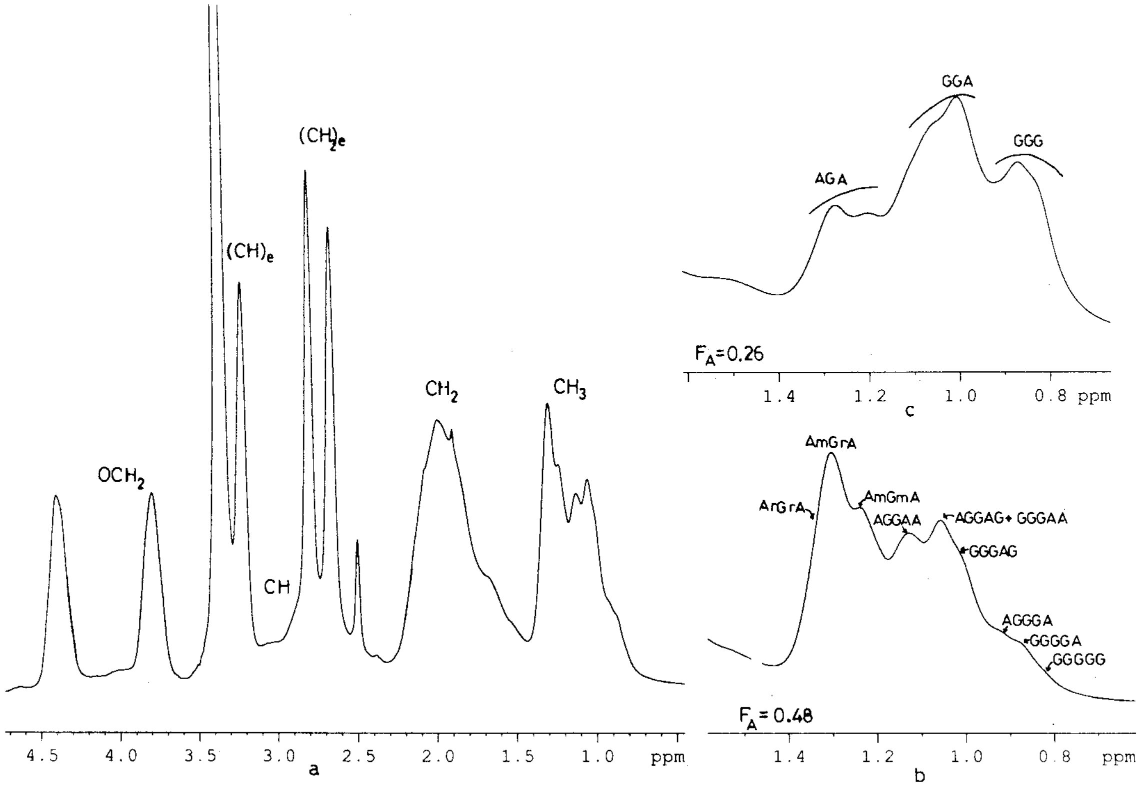

**Figure 6.** 300 MHz $^1$H NMR spectrum of acrylonitrile/glycidyl methacrylate copolymer (a) $F_A = 0.48$ and the expanded $CH_3$ region of (b) $F_A = 0.48$ and (c) $F_A = 0.26$.

AAAG (GAAA) ($\delta$ 34.85 ppm), and GAAG ($\delta$ 36.36 ppm) tetrads (Figure 3). The hexad compositional sequence in the GAAG centered tetrad are assigned at $\delta$ 36.29/2.03 (AGAAGG) and 36.49/1.89 (GGAAGG) ppm.

The AG(GA) diad can also be divided into three tetrad AAGA ($\delta$ 38.5−41.4 ppm), AAGG + AGAG ($\delta$ 41.4−43.1 ppm), and GAGG ($\delta$ 43.1−44.6 ppm), as shown in Figure 3. The splitting patterns within these tetrads are complex and overlapping, and further assignments are difficult. The three GG-centered tetrads AGGA, AGGG, and GGGG are assigned around $\delta$ 44.8−46.7, 46.7−50.5, and 50.0−55.0 ppm, respectively, on the basis of change in signal intensity with copolymer composition. Further splittings in the AGGG and GGGG tetrads are assigned to hexad sequences, with the help of the inverse-HETCOR spectrum. From the inverse-HETCOR spectrum (Figure 5b), the cross-peaks at $\delta$ 47.65/2.11, 48.67/2.06 (48.71/2.19), and 50.34/2.04 ppm are assigned to

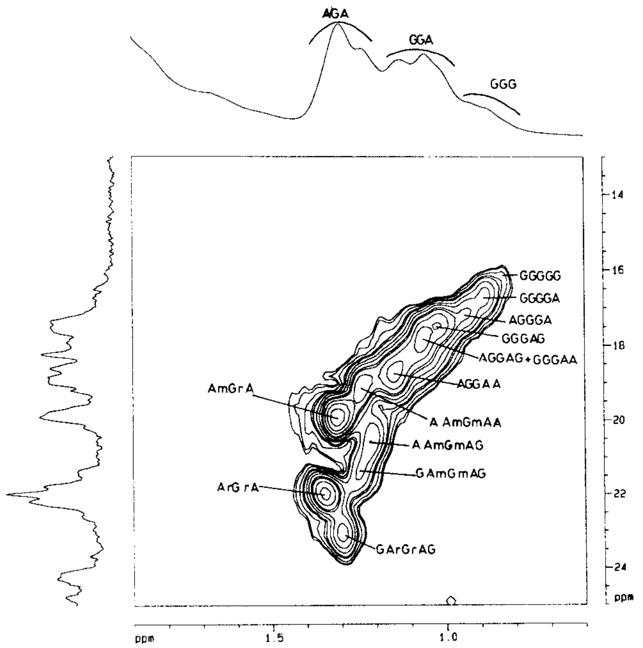

**Figure 7.** Methyl region of the inverse-HETCOR spectrum of A/G copolymer ($F_A$ = 0.48).

AGGG-centered AAGGGA, AAGGGG + GAGGGA, and GAGGGG hexad sequences, respectively. The three GGGG-centered hexad sequences are assigned at $\delta$ 50.34/2.02 (AGGGGA), 51.49/2.00 (51.49/2.09) (AGGGGG), and 53.12/1.92 (GGGGGG) ppm. The cross-peaks at $\delta$ 52.84/1.97, 53.12/1.92, and 53.25/1.88 ppm can be assigned to configurational sequences in the GGGGGG hexad. The central methylene protons of AAGGGG and AGGGGG are nonequivalent and show two cross-peaks in the proton axis.

The methyl carbon signals overlap with the methine carbon signals, which can be resolved by DEPT experiments. However, the nonoverlapping methyl proton signals could be clearly assigned around $\delta$ 0.60−1.5 ppm and show both compositional and configurational sensitivity. The methyl proton region can be split into three broad envelopes that vary with copolymer composition and are assigned to AGA ($\delta$ 1.19−1.5 ppm), GGA (AGG) ($\delta$ 0.98−1.19 ppm), and GGG ($\delta$ 0.80−0.98 ppm), as shown in Figure 6b,c. These triad fractions further show signals that can be assigned to configurational or compositional sequences. In the GGG triad region, the signals at $\delta$ 1.06, 0.88, and 0.83 ppm are assigned to AGGGA, GGGGA (AGGGG), and GGGGG pentad sequences on the basis of change in intensity with copolymer composition. These assignments can also be confirmed by an inverse-HETCOR spectrum (Figure 7) where the cross-peaks at $\delta$ 17.00/1.06, 16.51/0.88, and 16.06/0.83 ppm are assigned to these three GGG-centered pentads, respectively. Similarly, in the AGG (GGA) triad region, the three GGA-centered pentads are assigned at $\delta$ 18.61/1.14 (AGGAA), 17.79/1.06 (AGGAG + GGGAA), and 17.36/1.02 (GGGAG) ppm, as shown in Figure 7. The signals in the AGA triad region, which do not change with copolymer composition, are assigned to AmGmA ($\delta$ 1.24 ppm), AmGrA (ArGmA) ($\delta$ 1.31 ppm), and ArGrA ($\delta$ 1.35 ppm). Further compositional sequences within these triads are assigned with the help of the inverse-HETCOR spectrum, as shown in Figure 7. Thus with the help of the inverse-HETCOR experi-

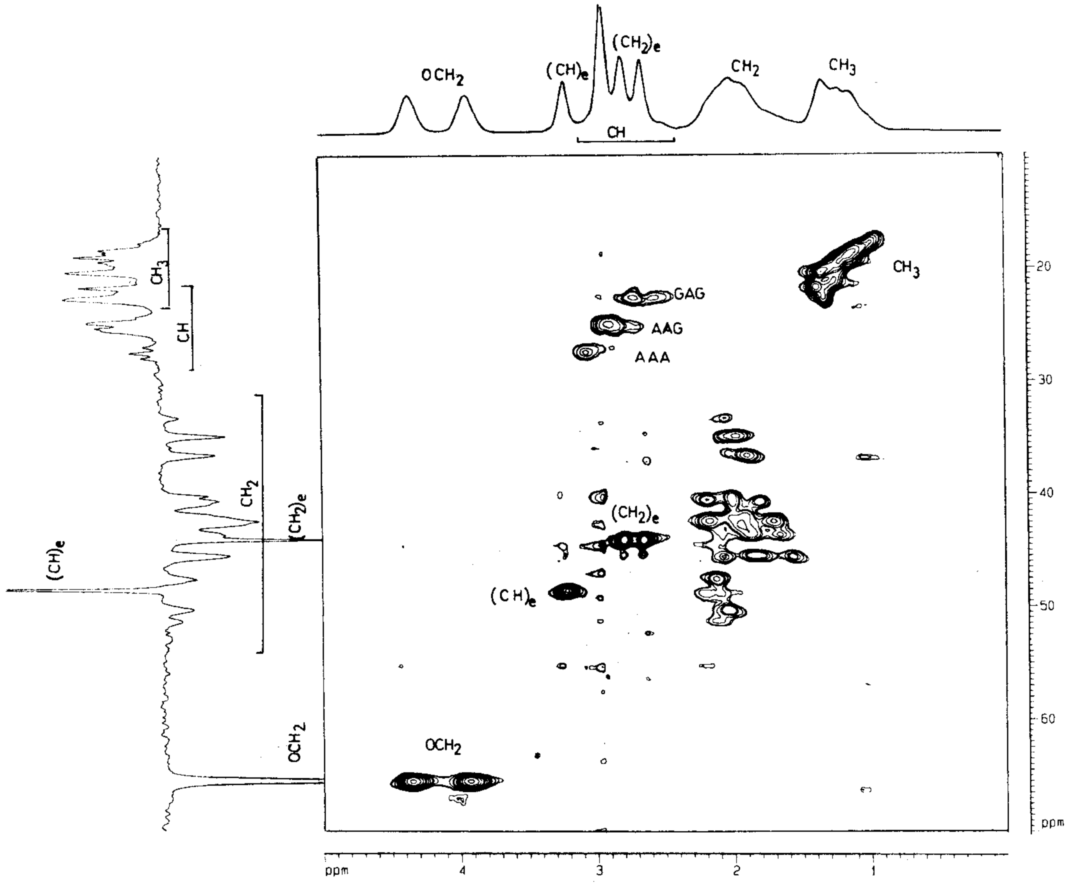

**Figure 8.** Inverse-HETCOR spectrum of the A/G copolymer ($F_A$ = 0.48) in DMSO-$d_6$ at 100 °C.

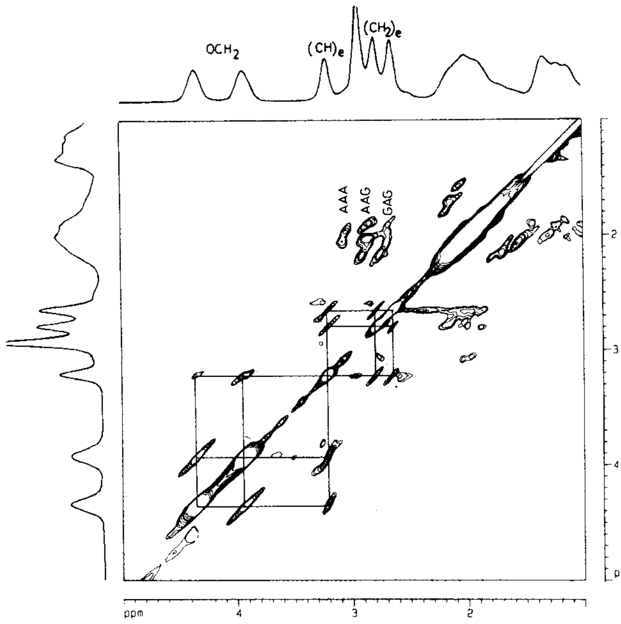

**Figure 9.** 2D TOCSY spectrum of the A/G copolymer ($F_A$ = 0.48) recorded in DMSO-$d_6$ at 100 °C.

**Table 1. Feed Mole Fraction, Copolymer Composition, and the Percent Nitrogen of the Acrylonitrile/Glycidyl Methacrylate Copolymers (A/G)**

| s. no. | feed mole fraction $f_A$ | percent conversion | percent nitrogen | copolymer composition $F_A$ | theoretical composition $F_A$ |
|---|---|---|---|---|---|
| 1 | 0.95 | 6.5 | 16.49 | 0.82 | 0.83 |
| 2 | 0.90 | 5.2 | 12.82 | 0.72 | 0.72 |
| 3 | 0.85 | 6.2 | 10.31 | 0.63 | 0.64 |
| 4 | 0.80 | 4.8 | 9.06 | 0.58 | 0.58 |
| 5 | 0.75 | 5.8 | 7.65 | 0.52 | 0.53 |
| 6 | 0.70 | 4.2 | 6.81 | 0.48 | 0.48 |
| 7 | 0.65 | 6.3 | 6.25 | 0.45 | 0.44 |
| 8 | 0.60 | 5.9 | 5.50 | 0.41 | 0.40 |
| 9 | 0.55 | 6.0 | 4.64 | 0.36 | 0.37 |
| 10 | 0.40 | 6.5 | 2.99 | 0.26 | 0.27 |

**Table 2. Triad Compositions Calculated from NMR Spectra, Monte Carlo Simulations and Alfrey-Mayo Model in Acrylonitrile/Glycidyl Methacrylate (A/G) Copolymers**

| s. no. | feed mole fraction of A | triads | triad concn[a] $^{13}C\{^1H\}$ NMR | Alfrey-Mayo | Monte Carlo |
|---|---|---|---|---|---|
| 1. | 0.95 | AAA | 0.64 | 0.65 | 0.78 |
| | | AAG | 0.29 | 0.31 | 0.20 |
| | | GAG | 0.07 | 0.04 | 0.02 |
| | | GGG | | 0.01 | |
| | | GGA | 0.15 | 0.13 | 0.07 |
| | | AGA | 0.85 | 0.86 | 0.93 |
| 2. | 0.90 | AAA | 0.47 | 0.44 | 0.57 |
| | | AAG | 0.44 | 0.45 | 0.37 |
| | | GAG | 0.09 | 0.11 | 0.06 |
| | | GGG | 0.02 | 0.02 | 0.01 |
| | | GGA | 0.23 | 0.24 | 0.15 |
| | | AGA | 0.75 | 0.74 | 0.84 |
| 3. | 0.85 | AAA | 0.33 | 0.31 | 0.37 |
| | | AAG | 0.50 | 0.49 | 0.48 |
| | | GAG | 0.17 | 0.20 | 0.15 |
| | | GGG | 0.06 | 0.04 | 0.02 |
| | | GGA | 0.31 | 0.33 | 0.22 |
| | | AGA | 0.63 | 0.63 | 0.76 |
| 4. | 0.80 | AAA | 0.23 | 0.22 | 0.21 |
| | | AAG | 0.52 | 0.50 | 0.50 |
| | | GAG | 0.25 | 0.28 | 0.29 |
| | | GGG | 0.08 | 0.07 | 0.03 |
| | | GGA | 0.35 | 0.39 | 0.29 |
| | | AGA | 0.57 | 0.54 | 0.68 |
| 5 | 0.75 | AAA | 0.15 | 0.16 | 0.12 |
| | | AAG | 0.49 | 0.48 | 0.45 |
| | | GAG | 0.36 | 0.36 | 0.43 |
| | | GGG | 0.11 | 0.11 | 0.05 |
| | | GGA | 0.44 | 0.44 | 0.36 |
| | | AGA | 0.45 | 0.45 | 0.59 |
| 6 | 0.70 | AAA | 0.11 | 0.12 | 0.07 |
| | | AAG | 0.45 | 0.45 | 0.40 |
| | | GAG | 0.44 | 0.43 | 0.53 |
| | | GGG | 0.17 | 0.15 | 0.10 |
| | | GGA | 0.52 | 0.47 | 0.42 |
| | | AGA | 0.31 | 0.38 | 0.48 |
| 7 | 0.65 | AAA | 0.10 | 0.09 | 0.05 |
| | | AAG | 0.39 | 0.41 | 0.33 |
| | | GAG | 0.51 | 0.50 | 0.62 |
| | | GGG | 0.17 | 0.19 | 0.15 |
| | | GGA | 0.52 | 0.49 | 0.47 |
| | | AGA | 0.31 | 0.32 | 0.38 |
| 8 | 0.60 | AAA | 0.05 | 0.06 | 0.03 |
| | | AAG | 0.38 | 0.38 | 0.28 |
| | | GAG | 0.57 | 0.56 | 0.69 |
| | | GGG | 0.23 | 0.24 | 0.22 |
| | | GGA | 0.51 | 0.50 | 0.50 |
| | | AGA | 0.26 | 0.26 | 0.28 |
| 9 | 0.55 | AAA | 0.05 | 0.05 | 0.02 |
| | | AAG | 0.32 | 0.33 | 0.24 |
| | | GAG | 0.63 | 0.62 | 0.74 |
| | | GGG | 0.30 | 0.29 | 0.32 |
| | | GGA | 0.47 | 0.50 | 0.49 |
| | | AGA | 0.23 | 0.21 | 0.19 |
| 10 | 0.40 | AAA | 0.02 | 0.02 | 0.01 |
| | | AAG | 0.23 | 0.22 | 0.14 |
| | | GAG | 0.75 | 0.76 | 0.85 |
| | | GGG | 0.49 | 0.47 | 0.58 |
| | | GGA | 0.44 | 0.43 | 0.36 |
| | | AGA | 0.07 | 0.10 | 0.06 |

[a] A- and G-centered triad fractions add up to unity.

ment, overlapping methyl carbon signals can be assigned without ambiguity.

The other proton signals in the $^1H$ NMR spectrum (Figure 6) are overlapping. From the one to one correlation between the carbon and proton signals in the inverse-HETCOR spectrum (Figure 8), the complex $^1H$ NMR spectrum was completely assigned. The $-OCH_2$ protons which are adjacent to the chiral center show diastereomerism and give two cross-peaks at $\delta$ 65.48/4.35 and 65.48/3.93 ppm. Similarly, epoxy methylene $(CH_2)_e$ protons also give two cross-peaks at $\delta$ 44.04/2.80 and 44.04/2.65 ppm. The epoxy methine proton is assigned at $\delta$ 3.22 ppm, which shows a heteronuclear correlation with the carbon at $\delta$ 48.60 ppm. The main chain methine proton shows triad sensitivity but is overlapped with the epoxy methylene protons. From Figure 8, the three triad fractions are assigned at $\delta$ 3.09−3.00 (AAA), $\delta$ 3.00−2.72 (AAG), and $\delta$ 2.72−2.53 (GAG) ppm. The methine proton of these triad fractions shows three-bond coupling with the methylene protons, which are seen in the low mixing time TOCSY spectrum (4 ms), apart from the other three-bond couplings between the various other protons (Figure 9).

The expanded $^{13}C\{^1H\}$ NMR spectra of the nitrile and carbonyl carbon resonance of the A/G copolymer are shown in Figure 2. In the nitrile region, the signals around $\delta$ 119.0−120.3, 120.3−121.7, and 121.7−124.0 ppm are assigned to AAA, AAG (GAA), and GAG triads, respectively. In the carbonyl carbon region, the intensities of the signals around $\delta$ 173.5−174.95, 174.95−176.50, and 176.50−178.0 ppm, which change with the copolymer composition, are assigned to AGA, GGA (AGG), and GGG triad sequences. The relative concen-

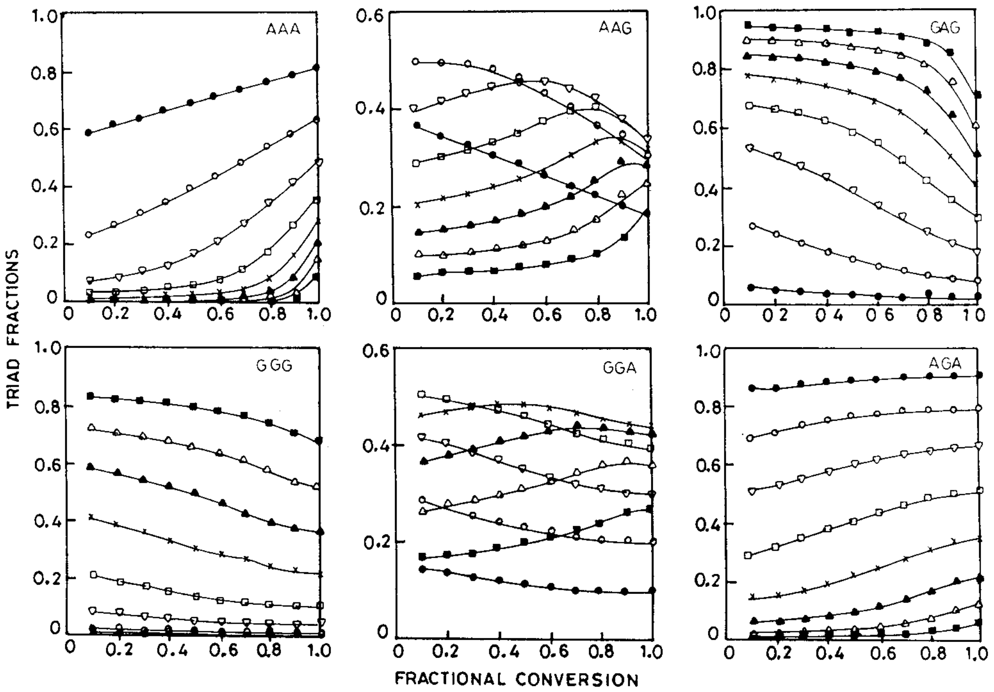

**Figure 10.** Variation of A- and H-centered triad fractions are plotted as a function of fractional conversion for different feed mole fractions: $f_A = 0.90$ (●); $f_A = 0.80$ (○); $f_A = 0.75$ (▽); $f_A = 0.70$ (□); $f_A = 0.60$ (×); $f_A = 0.50$ (▲); $f_A = 0.40$ (△); $f_A = 0.30$ (■).

trations of various A- and G-centered triads were obtained from the normalized areas of their resonance signals. The microstructure of A/G copolymers in terms of the A- and G-centered triad sequence distribution from $^{13}C\{^1H\}$ NMR spectra was found to be in good agreement with the theoretical values calculated by the Harwood program[22] and Monte Carlo simulation, using terminal model reactivity ratios $r_A = 0.22$ and $r_G = 1.44$ (Table 2). The correlation coefficient calculated between the triad fractions obtained from NMR spectroscopy and those calculated from the Alfrey-Mayo model and Monte Carlo simulations are 0.995 and 0.966, respectively.

The conditional probabilities[23] $P_{G/A}$ and $P_{A/G}$ were calculated from the triad concentrations determined from NMR spectroscopy. The values of $P_{G/A}$ increase linearly from 0.22 to 0.86, while the value of $P_{A/G}$ decreases from 0.92 to 0.29 as the acrylonitrile content in the copolymer decreases. Using these conditional probabilities, terminal model reactivity ratios were calculated for different feed mole fractions. The average value of the reactivity ratios are $r_A = 0.23 \pm 0.02$ and $r_G = 1.52 \pm 0.15$, which are within the experimental error.

**Monte Carlo Simulation Studies.** The MC simulation method can be used to determine the triad fractions at various degrees of polymerization. The detailed methodology of the MC simulation is given elsewhere.[18] Figure 10 shows the variation of the A- and G-centered triad concentrations as a function of fractional conversion for different feed mole fractions. The AAA triad fraction is seen to increase as the conversion increases. As the $f_A$ decreases, the triad fraction (AAA) increases only at higher conversion as glycidyl methacrylate is consumed faster than acrylonitrile comonomer. The AAG triad fraction concentration first increases, goes through a maximum, and then decreases as the conversion increases. The maximum shifts toward higher conversion as $f_A$ decreases. For $f_A > 0.80$ and $f_A < 0.20$ there is only a steady decrease and increase of the AAG triad concentration as the fractional conversion increases. The GAG triad fraction decreases as the fractional conversion increases. Glycidyl methacrylate has higher reactivity ratios and $f_G$ is higher so the GAG triad fraction is formed initially but at a higher conversion it decreases very sharply as glycidyl methacrylate is consumed faster. The GGG triad concentration decreases as the fractional conversion increases. The GGA triad fraction, for the feed mole fraction between $0.70 > f_A > 0.10$, increases, goes through a maximum, and then decreases as the fractional conversion increases. The AGA triad fraction increases as the fractional conversion increases.

## Conclusion

The reactivity ratios of the A/G copolymer system are $r_A = 0.22$ and $r_G = 1.44$. The overlapping and broad signals in the carbon and proton spectra were assigned completely to various compositional and configurational sequences with the help of inverse-HETCOR and TOCSY experiments. The methine and methyl carbon resonances were assigned to pentad sequences. The methylene carbon resonances were assigned to tetrad and hexad sequences with the help of the inverse HETCOR experiments. The copolymerization mechanism of the A/G copolymers were found to follow the first-order Markov model.

**Acknowledgment.** The authors wish to thank the Department of Chemistry, Indian Institute of Technology, Delhi, for providing the necessary funds and the NMR facility to carry out this work.

## References and Notes

(1) Mark, H. F.; Bikales, N. M.; Overberger, C. G.; Menges, G. *Encylopedia of Polymer Science and Engineering;* Wiley-Interscience: New York, 1985; Vol. 1, p 461.

(2) Vogl, O. *Makromol. Chem. Macrmol. Symp.* **1987**, *12*, 351.

(3) Webster, O. W.; Sogah, D. Y. In *Recent Advances in Mechanistic and Synthetic Aspects of polymerization.* Fontanille, M.,

Guyot, A., Eds.; Riedel Publishing Co.: Dodrecht, Netherlands, 1987.

(4) Kalal, J.; Svec, F.; Marousek, V. *J. Polym. Sci. Symp.* **1974**, *47*, 155.

(5) Tomalia, D. A. In *Functional Monomers;* Yocum, R. H., Nuquist, E. B., Eds.; Dekker: New York, 1974; Vol. 2.

(6) Frechet, J. M. J.; Bald E.; Svec, F. *React. Polym.* **1985**, *1*, 21.

(7) Lindsay, D.; Sherrington, D. C. *React. Polym.* **1985**, *3*, 27.

(8) Dhal, P. K.; Babu, G. N.; Sudhakaran, S.; Borkar, P. S. *J. Polym. Sci., Polym. Chem. Ed.* **1985**, *23*, 319.

(9) Dhal, P. K.; Babu, G. N.; Sudhakaran S.; Borkar, P. S. *Makromol. Chem. Rapid. Commun.* **1985**, *6*, 91.

(10) Thomson, F. L.; Yau L.; Doerries, E. M. *J. Electrochem. Soc.* **1979**, *126*, 1703.

(11) Dhal, P. K.; Babu, G. N.; Steigel, A. *Polymer* **1989**, *30*, 1530.

(12) Hunter, T. C.; Price, G. J. *Polymer* **1994**, *35*, 3530.

(13) Dhal, P. K.; Babu, G. N.; Nanda, R. K. *Macromolecules* **1984**, *17*, 1131.

(14) Brar, A. S.; Shiv Charan, *J. Polym. Sci., Part A: Polym. Chem.* **1996**, *34*, 333.

(15) (a) Guillot, J.; Guyot, A.; Pham, Q. T. *J. Macromol. Sci. Chem.* **1968**, *2*, 1303. (b) Guyot, A.; Guillot, J. *J. Macromol. Sci. Chem.* **1968**, *2*, 889. (c) Cattiaux, J.; Suzuki, T.; Harwood, H. J. *J. Appl. Polym. Sci., Polym. Symp.* **1978**, *1*, 34. (d) Brar, A. S.; Dutta, K.; Hekmatyar, S. K. *J. Polym. Sci., Part A: Polym. Chem.* **1998**, *36*, 1081. (e) Kapur, G. S.; Brar, A. S. *Makromol Chem*, **1991**, *192*, 2733.

(16) Kelen, T.; Tudos, F. *J. Macromol. Sci. Chem.* **1975**, *A9*, 1.

(17) Dube, M.; Sanyel, R. A.; Penlidis, A.; O'Driscoll, K. F.; Reilly, P. M. *J. Polym. Sci., Polym. Chem. Ed.*, **1991**, *29*, 703.

(18) Brar, A. S.; Jayaram B.; Dutta, K. *J. Polym. Mater.* **1993**, *10*, 269.

(19) Bodenhauser, G.; Ruben, D. J. *Chem. Phys. Lett.* **1980**, *69*, 185.

(20) van Herk, A. M. *J. Chem. Educ.* **1995**, *72*, 138.

(21) Gerken, T. A.; Ritchey, W. M. *J. Appl. Polym. Sci., Appl. Polym. Symp.* **1978**, *34*, 17.

(22) Harwood: H. J. *J. Polym. Sci. C* **1968,** *25*, 37.

(23) Koenig, J. L. *Chemical Microstructure of Polymer Chains;* Wiley-Interscience: New York, 1980.

MA980184Q